Title

Perm1 enhances mitochondrial biogenesis, oxidative capacity, and fatigue resistance in adult skeletal muscle

Journal

The FASEB Journal, 30(2)

ISSN

0892-6638

Authors

Cho, Yoshitake
Hazen, Bethany C
Gandra, Paulo G
et al.

Publication Date

2016-02-01

DOI

10.1096/fj.15-276360

Peer reviewed

The FASEB Journal article fj.15-276360. Published online October 19, 2015.

Perm1 enhances mitochondrial biogenesis, oxidative capacity, and fatigue resistance in adult skeletal muscle

Yoshitake Cho,* Bethany C. Hazen,* Paulo G. Gandra,* Samuel R. Ward,† Simon Schenk,† Aaron P. Russell,‡ and Anastasia Kralli*,[1]

*Department of Chemical Physiology, The Scripps Research Institute, La Jolla, California, USA; †Department of Orthopedic Surgery, School of Medicine, University of California, San Diego, La Jolla, California, USA; and ‡Centre for Physical Activity and Nutrition Research, School of Exercise and Nutrition Sciences, Deakin University, Burwood, Australia

ABSTRACT **Skeletal muscle mitochondrial content and oxidative capacity are important determinants of muscle function and whole-body health. Mitochondrial content and function are enhanced by endurance exercise and impaired in states or diseases where muscle function is compromised, such as myopathies, muscular dystrophies, neuromuscular diseases, and age-related muscle atrophy. Hence, elucidating the mechanisms that control muscle mitochondrial content and oxidative function can provide new insights into states and diseases that affect muscle health. In past studies, we identified *Perm1* (PPARGC1- and ESRR-induced regulator, muscle 1) as a gene induced by endurance exercise in skeletal muscle, and regulating mitochondrial oxidative function in cultured myotubes. The capacity of Perm1 to regulate muscle mitochondrial content and function *in vivo* is not yet known. In this study, we use adeno-associated viral (AAV) vectors to increase Perm1 expression in skeletal muscles of 4-wk-old mice. Compared to control vector, AAV1-Perm1 leads to significant increases in mitochondrial content and oxidative capacity (by 40–80%). Moreover, AAV1-Perm1–transduced muscles show increased capillary density and resistance to fatigue (by 33 and 31%, respectively), without prominent changes in fiber-type composition. These findings suggest that Perm1 selectively regulates mitochondrial biogenesis and oxidative function, and implicate Perm1 in muscle adaptations that also occur in response to endurance exercise.—Cho, Y., Hazen, B. C., Gandra, P. G., Ward, S. R., Schenk, S., Russell, A. P., Kralli, A. Perm1 enhances mitochondrial biogenesis, oxidative capacity, and fatigue resistance in adult skeletal muscle. *FASEB J.* 30, 000–000 (2016). www.fasebj.org**

Key Words: oxidative metabolism · angiogenesis · endurance exercise responses · skeletal muscle plasticity

Adult skeletal muscle shows remarkable plasticity, with many of its features and functional properties being shaped by the type and degree of physical exertion. For example, in response to endurance exercise training, muscle adapts with increases in mitochondrial content, oxidative capacity and vascularization, and changes in fiber-type composition (1). Conversely, physical inactivity, immobilization, aging, and many disease states are associated with decreases in muscle oxidative capacity and distinct changes in fiber-type composition (2–4). The skeletal muscle adaptations to physical activity (or inactivity) affect muscle performance and exercise tolerance, as well as whole-body health and well-being (5). Remarkably, genetic or pharmacologic manipulations that mimic exercise-induced adaptations in rodent skeletal muscle can also counteract the impact of diseases affecting muscle or aging. For example, transgene-mediated enhancement of oxidative capacity ameliorates symptoms of muscular dystrophy, myopathies, and aging in mouse models (6–9). Hence, elucidating the signaling networks that control skeletal muscle mitochondrial biogenesis and oxidative function is important for understanding the mechanisms that underlie muscle plasticity and enable adaptations, and for identifying novel targets for the treatment of diseases associated with muscle mitochondrial defects.

Endurance exercise induces intracellular signaling pathways, *via* the activation of the p38 MAPK, the AMPK, and Ca^{2+}-dependent kinases and phosphatases, such as CaMK and calcineurin (1, 10–12). These signal transducers control the activity and expression of transcriptional regulators [*e.g.*, ATF2, PGC-1 (peroxisome proliferator-activated receptor γ coactivator 1), NRF1 (nuclear respiratory factor 1), GABP (GA-binding protein), NFAT, MEF2s, PPARs (peroxisome proliferator-activated receptors), and ERRs (estrogen-related receptors)], which subsequently drive the expression of sets of nuclear genes important for the adaptive responses. The induction of mitochondrial biogenesis is generally

Abbreviations: AAV, adeno-associated virus; AAV1, adeno-associated virus, serotype 1; AMPK, AMP-activated protein kinase; CPT1, carnitine palmitoyltransferase 1; CS, citrate synthase; EDL, extensor digitorum longus; ERR, estrogen-related receptor; FCCP, carbonyl cyanide-4-(trifluoromethoxy)phenylhydrazone; FDB, flexor digitorum brevis; GABP, GA-binding protein;

(*continued on next page*)

[1] Correspondence: Department of Chemical Physiology, The Scripps Research Institute, 10550 N. Torrey Pines Road, La Jolla, CA 92037, USA. E-mail: kralli@scripps.edu

doi: 10.1096/fj.15-276360

This article includes supplemental data. Please visit *http://www.fasebj.org* to obtain this information.

thought to be under the control of the transcriptional coactivators PGC-1α and PGC-1β, which are recruited *via* NRF1, GABP, and ERRα to the promoters of nuclear genes encoding regulators of mitochondrial replication and transcription (*e.g.*, Tfam, Tfb1m, and Tfb2m), components of the tricarboxylic acid cycle and oxidative phosphorylation (OxPhos) systems, and many other proteins important for mitochondrial biogenesis and oxidative function (13, 14). The coactivators PGC-1α and PGC-1β and the nuclear receptors ERRα and ERRγ also drive skeletal muscle angiogenesis, at least in part *via* the induction of *Vegfa* (15–17). Changes in fiber-type composition are thought to be primarily under the control of NFAT, though they are also controlled by PGC-1α, PGC-1β, PPARδ, and ERRβ/ERRγ (17–24). Notably, many of these transcriptional regulators seem to work as a tightly knit network, crosstalking and regulating each other's expression. For example, ATF2, MEF2, and PPAR factors regulate PGC-1α expression, whereas PGC-1α and ERRα regulate ERRα, PPARα, NRF1, and GABP expression (25–31), suggesting the presence of feed-forward regulatory loops that get activated to coordinate appropriate responses to exercise.

All of the regulators implicated so far in exercise-induced responses are present at high levels in skeletal muscle but are also expressed in multiple other tissues. The extent to which muscle may have tissue-specific factors regulating mitochondrial biogenesis in response to exercise has not yet been addressed. In our previous study, we identified Perm1 (PPARGC1- and ESRR-induced regulator, muscle 1) as a protein with a remarkably muscle-specific expression, induced by PGC-1α and ERRα, and required for the enhancement of oxidative capacity by PGC-1α in cultured myotubes (32). Besides skeletal and cardiac muscles, where its expression is very high, Perm1 is detectable only in brown adipose tissue, a depot that shares developmental and expression similarities to muscle (33). Skeletal muscle Perm1 levels are induced by endurance exercise and decreased in disease states with decreased oxidative capacity, as seen in patients with amyotrophic lateral sclerosis (32). Our findings suggested that the induction of Perm1 may be part of the mechanism by which exercise (and PGC-1/ERRs) regulates mitochondrial oxidative function in muscle. Interestingly, Perm1 regulates the expression of only a subset of genes induced by PGC-1α or ERRγ expression in C2C12 myotubes, suggesting that Perm1 selectively functions in specific PGC-1/ERR-driven pathways (32). The ability of Perm1 to control mitochondrial biogenesis or other PGC-1/ERR pathways in adult skeletal muscle is so far unknown.

To address the function of Perm1 in adult skeletal muscle *in vivo*, we used adeno-associated viral (AAV) vectors to enhance Perm1 expression in specific muscles and determine the effect of increased Perm1 levels on mitochondrial content, oxidative capacity, and muscle functional properties. Our findings show that Perm1 is a potent positive regulator of mitochondrial biogenesis and oxidative capacity. Perm1 enhanced also muscle capillarity and fatigue resistance, without altering fiber-type composition.

MATERIALS AND METHODS

Generation of adeno-associated virus, serotype 1

The AAV1 (adeno-associated virus, serotype 1)-FLAG-Perm1 vector was produced by the Vector Core of the University of Pennsylvania (Philadelphia, PA, USA), using the plasmid pZac2.1/FLAG-Perm1 (pZac2.1 with an insert coding for the Perm1 protein with an N-terminal FLAG epitope) (32).

AAV1 injection and animal studies

C57BL/6J mice (TSRI breeding colony) were housed at constant temperature on a 12 h light-dark cycle and with free access to food and water. All experimental procedures were conducted according to protocols approved by the Institutional Animal Care and Use Committee of The Scripps Research Institute (Protocol number 14-0004). For i.m. injections of AAV vectors, mice (4 wk old) were anesthetized with isoflurane and injected with AAV1 vectors at the following doses: 2.5×10^{10} viral genomes when injecting the frontal area of tibialis anterior (TA)/extensor digitorum longus (EDL) muscles, and 1.0×10^{10} viral genomes for injections into the flexor digitorum brevis (FDB) muscle. Each mouse had 1 leg injected with AAV1-Perm1 and the contralateral leg injected with AAV1-LacZ as a control. Four weeks following the injections, mice were killed (~11 AM, unless indicated otherwise), and muscles were dissected and stored at −80°C (for processing of protein, DNA, and RNA), frozen in liquid nitrogen-cooled isopentane (for histology and immunohistochemistry), subjected to electrical stimulation (for measurements of force production), or dissociated to single fibers (for oxygen consumption measurements).

Histologic analyses and immunohistochemistry

Skeletal muscle samples were pinned to corkboard and frozen in liquid nitrogen-cooled isopentane (34). Cross-sections (10 μm thick) were cut from the midbelly of the TA muscle on a cryostat at −18°C (Microm HM500; Waldorf, Germany). To assess overall fiber morphology, serial sections were stained with hematoxylin and eosin (H&E), and images of AAV1-LacZ and AAV1-Perm1–transduced TA muscles from 4 mice were taken using a Zeiss Axiovert S100 fluorescence microscope (Carl Zeiss Microscopy, Jena, Germany). For succinate dehydrogenase (SDH) staining, sections were air dried for 30 min and then incubated in 100 mM Tris-HCl buffer containing 50 mM sodium succinate, 0.6 mM nitro blue tetrazolium, and 0.02 mM phenazine methosulfate for 20 min at 37°C. For immunostaining, sections were fixed with PBS containing 4% paraformaldehyde (PFA), followed by blocking in 5% goat serum, and incubation with, first, primary antibodies

(*continued from previous page*)

GAPDH, glyceraldehyde-3-phosphate dehydrogenase; Glut4, glucose transporter type 4; H&E, hematoxylin and eosin; MAPK, mitogen-activated protein kinase; MHC, myosin heavy chain; mtDNA, mitochondrial DNA; NRF1, nuclear respiratory factor 1; OCR, oxygen consumption rate; OxPhos, oxidative phosphorylation; Perm1, PPARGC1- and ESRR-induced regulator, muscle 1; PFA, paraformaldehyde; PGC-1, peroxisome proliferator-activated receptor γ coactivator 1; phospho, phosphorylated; PPAR, peroxisome proliferator-activated receptor; SDH, succinate dehydrogenase; Sirt, sirtuin; TA, tibialis anterior

[anti-laminin antibody (1:200 dilution, rabbit polyclonal; Sigma-Aldrich, St. Louis, MO, USA); anti-CD31 antibody (1:200 dilution, rat monoclonal; BD Biosciences, Franklin Lakes, NJ, USA); or mouse monoclonal antibodies against myosin heavy chain (MHC; 1:50 dilution; Developmental Studies Hybridoma Bank, Iowa City, IA, USA), as follows: anti-MHC type I (BA-F8), anti-MHC IIa (SC-71), anti-MHC IIx (6H1), or anti-MHC IIb (BF-F3)], and then, secondary antibodies [1:500 dilution of Alexa 594 goat anti-rabbit, Alexa 594 goat anti-rat, Alexa 488 goat anti-rabbit, or Alexa 488 goat anti-mouse IgG (Invitrogen, Life Technologies, Carlsbad, CA, USA)]. Laminin-stained sections were used to determine cross-sectional fiber area, using ImageJ (NIH, Bethesda, MD, USA) as previously described (34). CD31-stained sections were used to determine capillary density by counting the total number of capillaries (CD31-positive spots) in an entire muscle cross-section at 20× magnification using ImageJ and expressing data as capillaries per unit area of muscle (16).

Transmission electron microscopy

Transmission electron microscopy was performed using standard techniques (35). Briefly, TA muscles from 3 mice perfused with 4% PFA and 1.5% glutaraldehyde in 0.1 M cacodylate buffer were dissected, cut into small pieces (1 mm^2), and fixed overnight with 2.5% glutaraldehyde/2% PFA in 0.1 M phosphate buffer (pH 7.4). Samples were then washed in 0.1 M sodium cacodylate buffer and postfixed for 5 h with 1% OsO_4 in cacodylate buffer. Samples were dehydrated in a graded ethanol series and embedded in Epon/Araldite resin (Electron Microscopy Sciences, Hatfield, PA, USA) overnight. Ultrathin sections were obtained, contrasted with uranyl acetate/lead citrate, and examined with a Philips CM100 microscope (FEI, Hillsboro, OR, USA).

Reverse transcription and quantitative real-time PCR analysis

Total RNA was extracted from whole muscles using TRIzol reagent (Life Technologies), and cDNA was synthesized using the SuperScript II Reverse Transcription system (Invitrogen, Life Technologies), as published (36). Relative mRNA levels were determined by quantitative PCR using cDNA, gene-specific primers (**Table 1**), SYBR Green reagent (Affymetrix, Santa Clara, CA, USA), and normalization to levels of glyceraldehyde-3-phosphate dehydrogenase (GAPDH), as described (37).

DNA isolation and quantification

Total DNA was prepared from whole TA muscle, according to standard procedures (38), and digested with 100 μg/ml RNase A for 30 min at 37°C. The relative copy numbers of mitochondrial and nuclear genomes were determined by quantitative PCR with primers specific to the *CoxII* (mitochondrial) and *Dio3* (nuclear) genes (Table 1).

Western blot and antibodies

Whole muscles were homogenized in lysis buffer containing 20 mM Tris-HCl (pH 7.8), 150 mM NaCl, 1 mM Na_3VO_4, 5 mM

TABLE 1. *Primers used for quantitative real-time PCR*

Gene	Forward primer	Reverse primer
Ckmt2	TGTCTGAGATGACGGAGCAG	CCTGGTGTGGTCTTCCTCAT
Glut4	GATTCTGCTGCCCTTCTGTCC	CGCTCTCTCTCCAACTTCCG
Fabp3	AAGTGGAACGGGCAGGAGA	GAGGAGCGGGCGGTCAG
Cpt1b	CTCCGAAAAGCACCAAAACAT	AGGCTCCAGGGTTCAGAAAGT
ERRα	GGAGGACGGCAGAAGTACAAA	GCGACACCAGAGCGTTCAC
ERRβ	ACATTGCCTCTGGCTACCAC	CCCACTTTGAGGCATTTCAT
ERRγ	TCCCCGACAGTGACATCAAA	GTGTGGAGAAGCCTGGAATA
PPARα	AAGGCTATCCCAGGCTTTGC	TTTAGAAGGCCAGGCCGATCTC
PPARδ	GTATGCGCATGGGACTCAC	GTCTGAGCGCAGATGGACT
Pdk4	GTTCCTTCACACCTTCACCAC	CCTCCTCGGTCAGAAATCTTG
PGC-1α	TGCCATTGTTAAGACCGA	GGTCATTTGGTGACTCTGG
PGC-1β	AGTGGGTGCGGAGACACAGAT	AAAGCTCCACCGTCAGGGACT
Sirt3	TTTCTTTCACAACCCCAAGC	ACAGACCGTGCATGTAGCTG
mt-CoxII	TCTCCCCTCTCTACGCATTCTA	ACGGATTGGAAGTTCTATTGGC
mt-CoxIII	TAGCCTCGTACCAACACATGA	AGTGGTGAAATTCCTGTTGGA
Dio3	GGAGGTTGTCCGACCTGAT	GTCCCTTGTGCGTAGTCGAG
Tfam	CAAAGGATGATTCGGCTCAG	AAGCTGAATATATGCCTGCTTTTC
Tfb1m	ACCGAGGGCTTGGAATGTTA	TGGATCAATGTCTGCCAACTGT
Tfb2m	TTTGGCAAGTGGCCTGTGA	CCCCGTGCTTTGACTTTTCTA
Nrip1 (*RIP140*)	TCCCCGACACGAAAAAGAAAG	ACATCCATTCAAAAGCCCAGG
Lrp130	TTAGCAGTGAAACTTATAGCACCTTGAT	TTCAGTGTGAAGCCCTTGATGT
Endog	CCACCAATGCGGACTACC	AGGCATTCTGGTTGAGGTGT
Mb	CAGGAAGTCCTCATCGGTCT	CCATGCTTCTTCAGGTCCTC
Nrf1	CCACGTTGGATGAGTACACG	CTGAGCCTGGGTCATTTTGT
Gabp (*Nrf2*)	CCGCTACACCGACTACGATT	ACCTTCATCACCAACCCAAG
Vegfa	AACGATGAAGCCCTGGAGT	AGGTTTGATCCGCATGATCT
Myh1 (*MHCIIx*)	TCTGCAGACGGAGTCAGGT	TTGAGTGAATGCCTGTTTGC
Myh2 (*MHCIIa*)	GTCAAAGGAGGAGGAACAGCAGC	GTTGAGTGAATGCTTGCTTCCCC
Myh4 (*MHCIIb*)	TGGCCGAGCAAGAGCTAC	TTGATGAGGCTGGTGTTCTG
Myh7 (*MHCI*)	GCCAACTATGCTGGAGCTGATGCCC	GGTGCGTGGAGCGCAAGTTTGTCATAAG
Gapdh	TCAACGGGAAGCCCATCA	CTCGTGGTTCACACCCATCA

EDTA, 1% Triton X-100, 5 μl/ml protease inhibitor cocktail P8340 (Sigma-Aldrich), and 20 μg/ml PMSF. Protein lysates were resolved by SDS-PAGE and transferred to nitrocellulose membrane (Hybond-C Extra; GE Healthcare Life Sciences, Pittsburgh, PA, USA). Western blotting was performed using the following antibodies: anti-FLAG (Clone M2; Sigma-Aldrich); anti-PERM1 (anti-C1orf170; Sigma-Aldrich); anti-tubulin (#2184; Cell Signaling Technology, Danvers, MA, USA); anti-Rt/Ms Total OxPhos Complex Kit (Invitrogen, Life Technologies); anti-ERRα (ab76228; Abcam, Cambridge, MA, USA); anti-PGC-1α (29); anti-Sirt3 (sirtuin 3; #5490; Cell Signaling Technology); anti-Myoglobin (sc-25607; Santa Cruz Biotechnology, Santa Cruz, CA, USA); anti-phospho-p38 MAPK (#9211; Cell Signaling Technology); and anti-p38 MAPK (#9212; Cell Signaling Technology). Horseradish peroxidase-conjugated anti-mouse or anti-rabbit secondary antibodies were purchased from Bio-Rad (Hercules, CA, USA). The blots were developed using the Pierce ECL reagent (Thermo Fisher Scientific, Waltham, MA, USA).

Mitochondrial enzyme activity assays

Whole TA muscles were homogenized in 50 mM Tris-HCl (pH 7.4), 5 μl/ml protease inhibitor cocktail (P8340), and 20 μg/ml PMSF. Homogenates were centrifuged at 1000 *g* for 10 min (at 4°C), and the resulting supernatants were tested for the enzymatic activities of electron transfer chain complexes I–IV and citrate synthase (CS), as described (39).

Fiber-type composition analysis

TA muscle myosins were extracted and analyzed by electrophoresis and silver staining as described (40). Silver-stained gels were scanned and quantitated using ImageJ. TA cross-sections immunostained with antibodies to myosins were also used to determine fiber-type composition (41).

Isolation of single FDB fibers and oxygen consumption assay

Oxygen consumption of single FDB fibers was measured using the XFe96 Extracellular Flux Analyzer (Seahorse Bioscience, North Billerica, MA, USA), as described (42), with minor modifications. Briefly, FDB muscles were dissected and incubated with 2 ml dissociation media containing DMEM, 2% fetal bovine serum, 1 mM sodium pyruvate, 2 mM glutamine, and 4 mg/ml collagenase A (Roche Diagnostics Corporation, Indianapolis, IN, USA) for 3 h (at 37°C and 5% CO_2). FDB muscles were then triturated with a wide-bore (5–6 mm) fire-polished glass pipette to yield single FDB myofibers. After 10 passes of trituration, the muscles were returned to the incubator for 20–30 min. The process was repeated until 70–80% of the muscle was digested. Undigested FDB muscle and large debris were removed using forceps. Digested FDB fibers were cleaned by gravity sedimentation, as follows: fibers were transferred to a 15 ml tube filled with 10 ml culture medium containing DMEM, 2% fetal bovine serum, 1 mM sodium pyruvate, and 2 mM glutamine, using a wide-bore pipette, and allowed to settle for 20 min; media were then aspirated, and the process was repeated once more. Cleaned fibers were then transferred to a 35 mm culture dish without coating and 2 ml culture media, and allowed to recover overnight at 37°C and 5% CO_2. The next day, the fibers were collected, aliquoted in Seahorse Bioscience XFe96 cell culture microplates that had been coated with GF-reduced BD Matrigel (#356230; diluted 1:9 in DMEM; BD Biosciences), at a density of 20–30 fibers per well, and cultured overnight at 37°C and 5% CO_2. The following day, the fibers were exchanged to Seahorse Bioscience assay buffer [phenol red-free DMEM with 10 mM 4-(2-hydroxyethyl)-1-piperazineethanesulfonic acid (pH 7.4), 25 mM glucose, 10 mM sodium pyruvate, and 2 mM glutamine] and incubated for 1 h at 37°C before measuring oxygen consumption rates (OCRs), using the XFe96 Extracellular Flux Analyzer and as described (42). Images of all wells (at ×4 magnification) were used to determine the number of fibers in each well. Basal, uncoupled (in the presence of 1 μM oligomycin), and maximal [in the presence of 800 nM carbonyl cyanide-4-(trifluoromethoxy) phenylhydrazone; FCCP] OCRs were calculated by subtracting background rates (in the presence of 1 μM antimycin A and 1 μM rotenone), normalized by the number of fibers in each well, and expressed as OCR per 20 fibers. Data shown are the means ± SD of 6 AAV1-LacZ and 6 AAV1-Perm1–transduced FDB muscles, with each muscle OCR being the average of 6–12 replicate wells.

Cell culture

Primary myoblasts were isolated from 6- to 8-wk-old mice and differentiated to myotubes as described (43). Differentiated myotubes were infected on d 4 of differentiation with adenoviruses expressing LacZ (control) or Perm1 at multiplicity of infection 50 (32). Cells were harvested 24 h after infection.

Ex vivo muscle contractile function and fatigue resistance

Mice were anesthetized, and the muscle belly of the fifth digit of the EDL was dissected as described (44). Matched muscles from the same animal transduced with AAV1-LacZ or AAV1-Perm1 were analyzed. Muscles were mounted in a specialized muscle chamber continuously perfused with Ringer's solution [137 mM NaCl, 5 mM KCl, 2 mM $CaCl_2$, 24 mM $NaHCO_3$, 1 mM NaH_2PO_4, 11 mM glucose, 1 mM $MgSO_4$, and 0.01% tubocurarine chloride (pH 7.5)] at 25°C, bubbled with 100% O_2. One of the tendons was tied with 5-0 silk suture to the arm of a muscle lever system (model 300B; Aurora Scientific, Aurora, ON, Canada), and the other tendon was tied to a micromanipulator allowing control of muscle position and length. Muscles were electrically stimulated (Model S88; Astro-Med, West Warwick, RI, USA) *via* parallel platinum electrodes (~35 V, 300 ms train duration, 0.3 ms pulse duration) with single twitches to set the length for maximal twitch tension. After a 10 min rest, muscles were stimulated at different frequencies (1–120 Hz) with 120 s intervals between contractions to determine the force-frequency relationship. The force-frequency curves were fitted by a nonlinear regression equation, $P = P_{min} + (P_0 X^{nH} / F_{50}{}^{nH} + X^{nH})$, where P_{min} is the minimum tension developed, F_{50} is the midpoint of the curve (in hertz), and n_H is the Hill coefficient. After the force-frequency protocol, muscles rested for 10 min, and the fatigue resistance was determined by repeated isometric contractions at the calculated F_{50} frequency. During the fatigue protocol, rest intervals started at 4 s and progressively decreased every 1 min (to 3 and 2 s). Time to fatigue was defined as the time it took each muscle to reach 40% of the force generated in the first contraction of the fatigue protocol. Force development was normalized to the muscle physiologic cross-sectional area, calculated as described (44). EDL muscles were also analyzed by Western blot analysis for Perm1 and OxPhos protein expression, to confirm efficient transduction and Perm1 function.

Statistics

Data shown are means ± SD or SEM, as indicated, and were analyzed with a 2-tailed Student's *t* test for single variables. For comparisons between multiple variables, *P* values were determined using a 2-way ANOVA test, followed by a Bonferroni analysis.

RESULTS

Increasing muscle Perm1 expression does not affect muscle gross morphology or fiber size

Skeletal muscle Perm1 expression is induced in response to an acute endurance exercise bout, elevated in trained compared to untrained individuals and mice, and enriched in red/oxidative fiber-rich compared to white/glycolytic fiber-rich parts of muscle [(32, 45); Supplemental Fig. 1], suggesting that increased Perm1 levels could be driving or contributing to some of the exercise-induced adaptations. To determine the consequences of increasing Perm1 levels in adult skeletal muscle, in the absence of endurance exercise, we used AAV1 vectors to transduce muscle and achieve stable Perm1 transgene expression (46). First, we confirmed the efficiency of transduction by injecting an AAV1-green fluorescent protein vector into the frontal area of TA and EDL muscles. When analyzed 4 wk post-injection, >95% of TA and EDL fibers were green fluorescent protein positive, as reported by others (Supplemental Fig. 2) (46). Next, we injected 4-wk-old mice with AAV1-FLAG-Perm1 into the TA of 1 hind limb and the control AAV1-LacZ into the contralateral TA muscle. Four weeks later, FLAG-Perm1 was efficiently expressed, resulting in significantly increased levels of the slower migrating Perm1 protein isoform (arrow in **Fig. 1*A***). By use of an antibody that detects only the AAV-expressed protein, FLAG-Perm1 was detected in the AAV1-Perm1–transduced muscle but not the control AAV1-LacZ–transduced contralateral muscle, confirming that AAV1 vector expression stays restricted to the injected leg. The increased expression levels of Perm1 did not alter muscle weight or cause any morphologic changes, as judged by H&E staining (Fig. 1*B, C*). Myofiber cross-sectional area was also similar in LacZ- and Perm1-transduced muscles (Fig. 1*D, E*). Thus, AAV1-Perm1 leads to efficient increases in Perm1 expression in the TA muscle, and increased levels of Perm1 do not affect muscle gross morphology or fiber size.

Perm1 enhances mitochondrial biogenesis and oxidative activity in adult skeletal muscle

In previous studies, we found that Perm1 was required for the induction of mitochondrial biogenesis by PGC-1α in cultured myotubes (32). Thus, we next assessed the effect of increased Perm1 expression on skeletal muscle mitochondrial content and oxidative activity. As shown in **Fig. 2*A***, Perm1 overexpression resulted in an increase in skeletal muscle mitochondrial DNA (mtDNA) content. The increase in mtDNA copy number was accompanied by higher expression levels of genes encoded by the mitochondrial genome, *mt-CoxII*

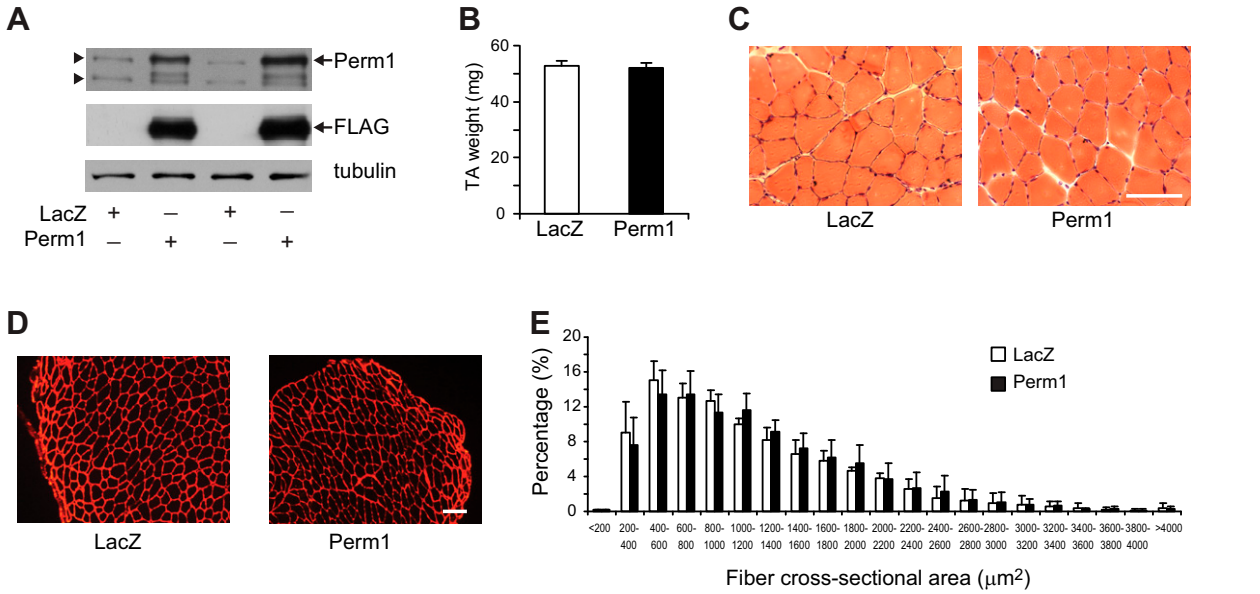

Figure 1. AAV1-mediated expression of Perm1 in TA muscle. AAV1 vectors expressing LacZ or FLAG-Perm1 were injected in the frontal area of TA muscles. After 4 wk, muscles were harvested. *A*) Perm1 protein levels were determined in muscle lysates by Western blotting, using antibodies against Perm1 (detecting endogenous and AAV1-expressed protein) and anti-FLAG (detecting only AAV1-expressed Perm1). The arrow on the right indicates the over-expressed Perm1 protein; arrowheads on the left indicate the 2 major protein forms encoded by endogenous Perm1 (32). Anti-tubulin antibodies were used to control for loading. *B*) Weights of TA muscles expressing LacZ or Perm1. Data are the means ± SD of 6 mice. *C* and *D*) Representative images of cross-sections of LacZ and Perm1 TA muscles stained with H&E (*C*) or immunostained with anti-laminin antibody (*D*). Scale bars, 100 μm. *E*) Distribution of fiber cross-sectional areas of LacZ and Perm1 TA muscles, calculated from laminin-stained images. Data are the means ± SD ($n = 4$ mice per group).

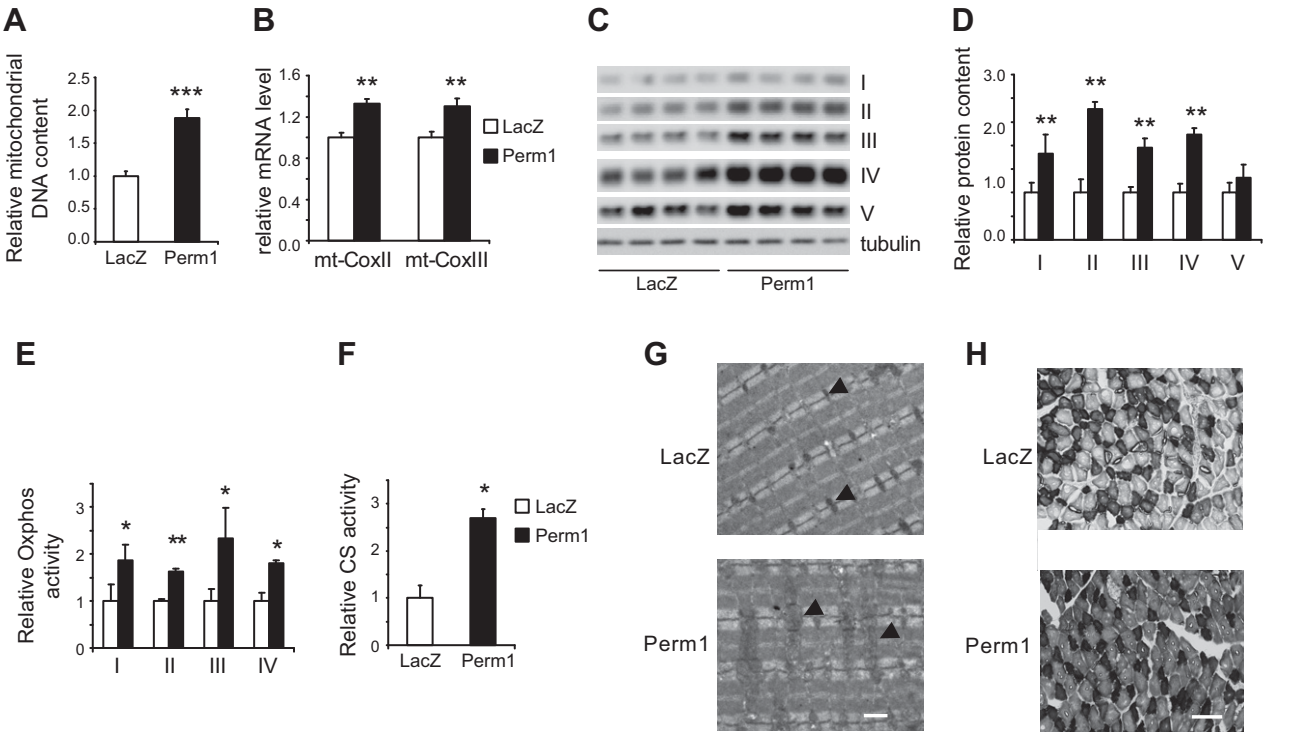

Figure 2. Perm1 enhances mitochondrial biogenesis and oxidative activity in skeletal muscle. *A*) The relative mtDNA content was determined as the ratio of mitochondrial (*CoxII*) to genomic (*Dio3*) DNA copy numbers, and expressed relative to the ratio seen in control (LacZ) TA muscles. *B*) mRNA levels for the indicated mitochondrial genome-encoded OxPhos genes were determined by RT-quantitative PCR, normalized to GAPDH levels, and expressed relative to levels of each gene in control (LacZ) TA muscles. *A* and *B*) Data are the means ± SE ($n = 14$). $^{**}P < 0.01$; $^{***}P < 0.001$. *C* and *D*) The levels of OxPhos complex proteins in TA muscles were determined by Western blot analysis, using total protein lysates and the Total OxPhos Complex antibody cocktail (*C*). The intensity of the bands was quantified using ImageJ software, and the values are expressed relative to the signal intensity in control (LacZ) TA muscles (*D*). Enzymatic activities of OxPhos complexes I–IV (*E*) and of CS (*F*) in total muscle lysates are shown. Data are the means ± SD, expressed relative to enzymatic activity in control (LacZ) TA muscles ($n = 4$). $^{*}P < 0.05$; $^{**}P < 0.01$. *G*) Representative transmission electron micrographs of LacZ and Perm1 TA muscles. Arrowheads indicate mitochondria. Scale bar, 1 μm. *H*) Representative images of cross-sections of LacZ and Perm1 TA muscles stained for SDH activity. Scale bar, 100 μm.

and *mt-CoxIII* (Fig. 2*B*), and significant increases in the abundance of mitochondrial OxPhos complexes (Fig. 2*C*, *D*). Consistent with the increase in OxPhos protein levels, Perm1 muscles showed a comparable increase in OxPhos complexes I–IV enzyme activity (Fig. 2*E*). Moreover, Perm1 muscles had significantly elevated levels of other mitochondrial enzymes important for oxidative metabolism, such as CS, an enzyme of the tricarboxylic acid cycle and commonly used marker of mitochondrial oxidative activity (Fig. 2*F*). The Perm1-induced increase in mitochondrial content was also observed by transmission electron microscopy of TA sections, where mitochondria appeared larger and at a higher density (Fig. 2*G*). Finally, *in situ* staining of TA sections for SDH showed higher SDH activity, with a pronounced SDH increase in the less oxidative (lighter-stained) fibers (Fig. 2*H*).

Perm1 increases muscle spare respiratory capacity

To assess the extent to which the increased mitochondrial content in Perm1 muscles leads to enhanced mitochondrial function and, in particular, respiratory capacity, we next compared oxygen consumption in Perm1 and control intact muscle fibers. For this, we administered the AAV1 vectors expressing FLAG-Perm1 or LacZ into the FDB muscles of 4-wk-old mice. As seen in the TA muscle, the increased Perm1 expression led to elevated protein levels of OxPhos complexes in FDB muscles (**Fig. 3*A***). Dissociated intact single FDB fibers were placed in matrix-coated Seahorse Bioscience XF96 plates (Fig. 3*B*), and oxygen consumption was measured in the absence and presence of drugs that enable assessment of different components of respiration (see Supplemental Fig. 3 for representative traces of OCRs). In the basal state (absence of any drugs), there was no difference in OCRs between control LacZ- or Perm1-over-expressing fibers, suggesting that Perm1 did not influence the basal energetic needs of muscle (Fig. 3*C*). Additionally, the increased Perm1 expression had no significant effect on oxygen consumption in the presence of oligomycin (inhibitor of ATP synthesis), suggesting that it did not alter the coupling of respiration to ATP synthesis. In contrast, Perm1 overexpression dramatically increased maximal OCRs (measured in the presence of the uncoupler FCCP) (Fig. 3*C*). These findings show that the increased

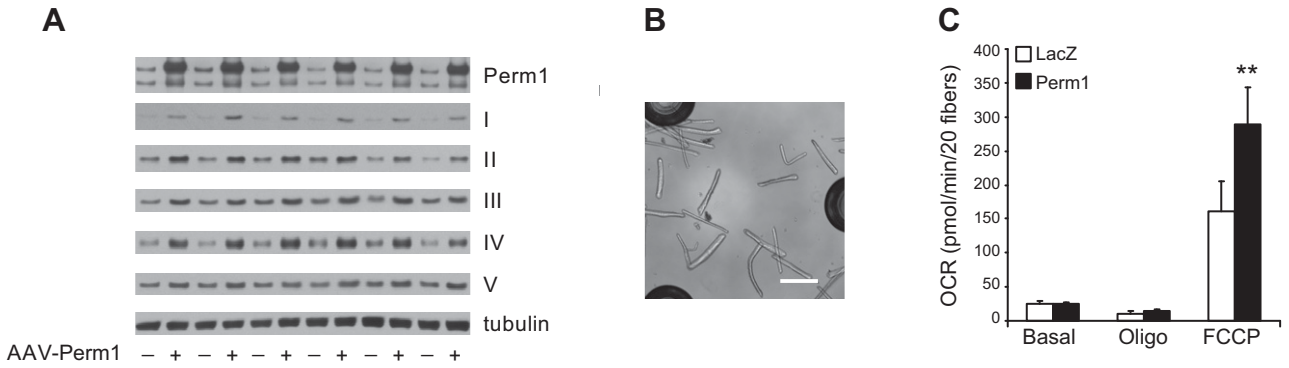

Figure 3. Perm1 increases spare respiratory capacity in muscle. FDB muscles were injected with AAV1 vectors expressing LacZ (−) or Perm1 (+) and dissected 4 wk later. *A*) Protein levels of Perm1 and OxPhos complexes in FDB muscles were determined by Western blotting, as in Figs. 1 and 2. *B*) A representative image of intact single FDB fibers cultured in a Seahorse Bioscience XFe96 plate. Scale bar, 600 μm. *C*) OCRs of intact single FDB fibers were measured in the absence and presence of 1 μM oligomycin and/or 800 nM FCCP. Rates are normalized by the number of fibers, corrected for nonmitochondrial oxygen consumption, and expressed as OCR per 20 fibers. The rates are the means ± SD of FDB fibers from 6 mice. $^{**}P < 0.01$.

mitochondrial content in Perm1-over-expressing muscles translates to higher oxidative capacity, with these muscles showing specifically higher spare respiratory capacity.

Increasing expression of Perm1 does not significantly alter fiber-type composition in TA muscles

The degree of mitochondrial content and oxidative capacity is characteristic of the different muscle fiber types: highest in type I slow-twitch and type IIa fast-twitch oxidative fibers, intermediate in type IIx fast-twitch mixed glycolytic/oxidative fibers, and lowest in IIb fast-twitch glycolytic fibers. Therefore, we next asked whether Perm1 affects the muscle fiber-type composition. First, we used high-resolution SDS-PAGE and silver staining to quantify the relative protein levels of the MHC isoforms that define fiber-type identity. As shown in **Fig. 4*A***, *B*, increasing Perm1 expression led only to a minor shift from IIb to IIa and IIx MHC content (2% of all MHCs), which whereas appearing significant in statistical terms ($P = 0.002$), is unlikely to have a significant physiologic impact on muscle function or to explain the marked increase in mitochondrial oxidative function. Next, we used staining of muscle cross-sections with antibodies against the different MHC isoforms to quantify the relative fiber-type content. Based on this approach, Perm1 had no effect on fiber-type composition (Fig. 4*C*, *D*). Both SDS-PAGE/silver staining and immunostaining confirmed the lack of type I fibers in LacZ- and Perm1-expressing TA muscles (Fig. 4*A*; data not shown). Moreover, we did not detect any significant changes in the mRNA levels of the genes encoding the different MHC isoforms (Fig. 4*E*), consistent with Perm1 having no prominent effect on fiber-type switching in adult skeletal muscle.

Increased expression of Perm1 enhances skeletal muscle vascularization

The signals that increase Perm1 expression (*i.e.*, endurance exercise, PGC-1α and PGC-1β, and ERRs) also increase angiogenesis, *via* the transcriptional induction of *Vegfa* (15–17). Thus, we next determined the effect of increased Perm1 expression on skeletal muscle capillary density, by staining TA muscle cross-sections with antibodies against platelet endothelial cell adhesion molecule-1 (CD31). We observed an ~30% increase in the number of CD31-positive endothelial cells in AAV1-FLAG Perm1-transduced muscle (**Fig. 5*A***, *B*) compared to control LacZ muscle, suggesting that Perm1 enhances vascularization. Consistent with the increase in capillary density, Perm1-over-expressing muscles had an increase in *Vegfa* mRNA content (Fig. 5*C*).

Perm1 remodels muscle p38 signaling and enhances the expression of select regulators of mitochondrial biogenesis and oxidative function

To gain insights into the pathways by which Perm1 remodels skeletal muscle, we next assessed the expression levels of genes known to be important for mitochondrial biogenesis and other aspects of skeletal muscle oxidative function. First, we assessed the mRNA levels of nuclear transcriptional regulators, including the coactivators of the PGC-1 family, the corepressor Rip140 (*Nrip1*), members of the ERR and PPAR subfamilies of nuclear receptors, and the DNA-binding transcription factors *NRF1* and *GABP*. As shown in **Fig. 6*A***, Perm1 led to increases in *PGC-1α* and *ERRα* mRNA levels. Next, we analyzed the expression of mitochondrial regulators and found that Perm1 led to increased expression of the mtDNA replication/transcription factors *Tfam* and *Tfb2m*, mitochondrial endonuclease *Endog*, and deacetylase *Sirt3* (Fig. 6*B*). The increases in PGC-1α, ERRα, and Sirt3 were confirmed at the protein level (Fig. 6*D*). In addition to regulators involved in mitochondrial biogenesis and function, Perm1 also led to increases of other genes known to be induced by endurance exercise and/or to be important for nutrient utilization and energy transduction, such as *Glut4* (glucose transporter type 4) and *Cpt1b* (carnitine palmitoyltransferase 1b) (Fig. 6*C*). For some genes, such as *Mb* (encoding myoglobin), Perm1 led to increased protein levels, even

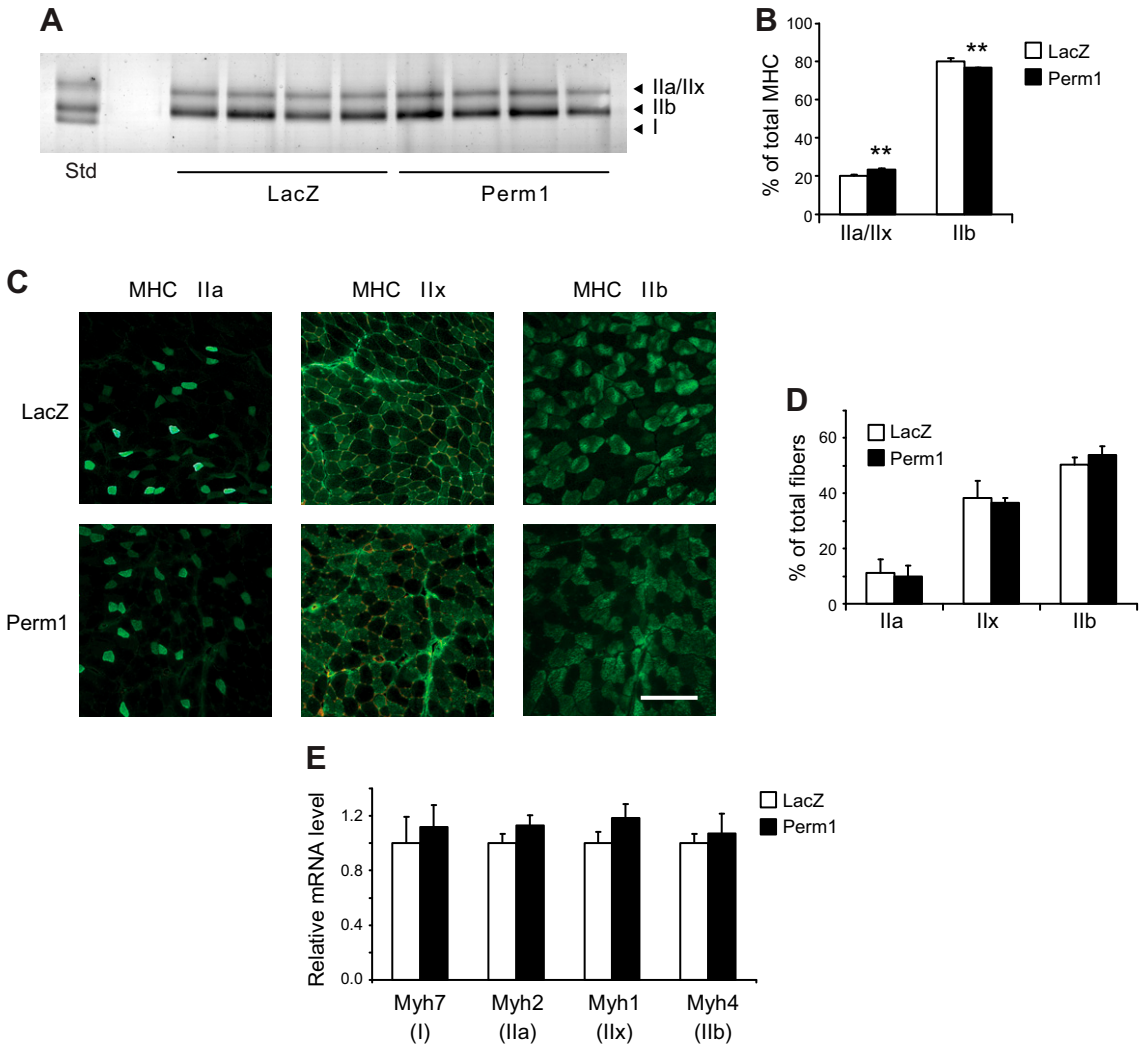

Figure 4. Perm1 does not alter fiber-type composition. *A*) MHC isoforms of control (LacZ) or Perm1 TA muscles were separated by SDS-PAGE and visualized by silver staining (125 ng skeletal muscle myosins per lane). Std, standard sample containing soleus (50%) and gastrocnemius (50%) muscle myosins was used as control for the migration pattern of all isoforms. *B*) The relative abundance of MHC isoforms in control (LacZ) and Perm1 TA muscles, based on quantification of myosin bands in (*A*) by ImageJ software. Data are expressed as percentages (%) of total MHCs and are the means ± SD ($n = 4$ mice per group). $^{**}P < 0.01$. *C*) Representative images of cross-sections show the midportion of LacZ and Perm1 TA muscles stained with antibodies against MHC isoforms, as indicated. Scale bar, 200 μm. *D*) The relative abundance of different fiber types in TA, based on quantitation of an entire TA section. Data are expressed as percentages (%) of total fibers and are the means ± SD ($n = 4$ mice per group). *E*) mRNA levels for the indicated MHC-encoding genes in TA muscles were determined by RT-quantitative PCR, normalized to GAPDH levels, and expressed relative to the levels of each gene in control (LacZ) muscle. Data are the means ± SE ($n = 14$).

though we did not detect an increase at the mRNA level (Fig. 6*C*, *D*).

Finally, we tested the extent to which Perm1 affected signaling pathways known to control mitochondrial biogenesis and responses to exercise. Comparison of AAV1-FLAG-Perm1 and control-transduced TA muscle lysates showed that the increase in Perm1 led to changes in the active [phosphorylated (phospho)] form of the MAPK p38. At daytime, when mice are resting, muscles with elevated Perm1 expression showed decreased levels of phospho-p38, whereas at nighttime, when mice are active, Perm1 muscles had significantly increased levels of phospho-p38 kinase (**Fig. 7** and Supplemental Fig. 4). To determine the acute effect of Perm1 on p38 in a system independent of diurnal changes, we next expressed Perm1 in primary myotubes. Perm1 led to an increase in the phosphorylated form of the p38 kinase (Fig. 7*C*). We did not detect differences in phospho- or total AMPK at any time (data not shown). These findings suggest that Perm1 induces a remodeling of skeletal muscle signaling pathways.

Perm1 expression enhances fatigue resistance in skeletal muscle

To gain better insight into the physiologic impact of the Perm1-induced skeletal muscle remodeling, we next compared the contractile and fatigue properties of isolated EDL muscles that had been transduced with either

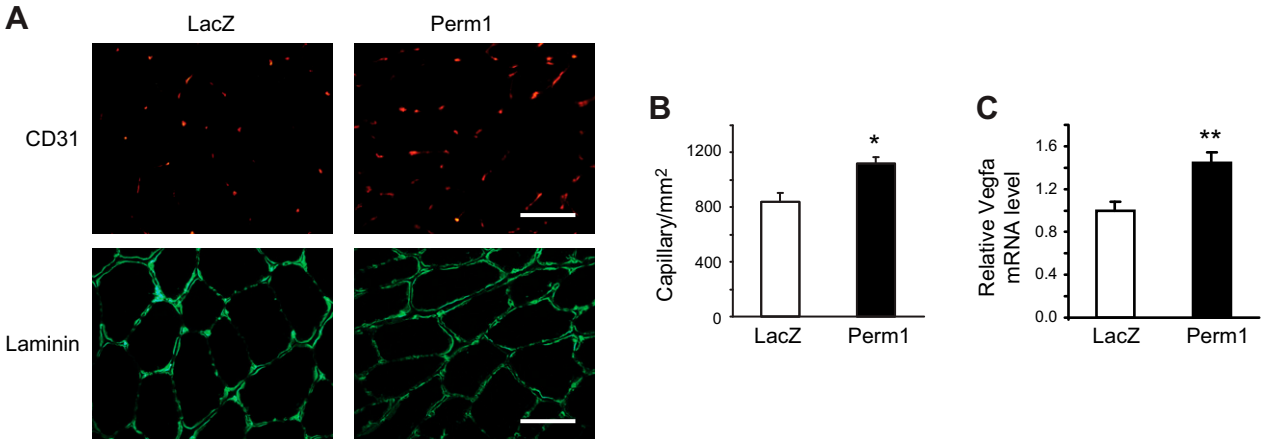

Figure 5. Increased expression of Perm1 enhances skeletal muscle vascularization. *A*) Representative images of cross-sections of LacZ and Perm1 TA muscles stained with anti-CD31 and anti-laminin antibodies. Scale bars, 50 μm. *B*) Capillary density of LacZ and Perm1 TA muscles, quantified from CD31-stained muscles, using ImageJ software. Data are the means ± SE ($n = 5$). *$P <$ 0.05. *C*) *Vegfa* mRNA levels were determined by RT-quantitative PCR, normalized to GAPDH levels, and expressed relative to the levels in control (LacZ) muscle. Data are the means ± SE ($n = 14$). **$P < 0.01$.

the AAV1-FLAG-Perm1 or AAV1-LacZ viruses. We found no significant differences in isometric force generation (at submaximal or maximal stimulation) or the rates of force generation and relaxation (**Fig. 8*A*** and **Table 2**), suggesting no changes in contractile properties. However, Perm1 muscles showed delayed fatigue (Fig. 8*B*, *C*), suggesting that the increased Perm1 levels confer resistance to fatigue.

DISCUSSION

We previously identified Perm1 as a PGC-1α/β and ERR-induced gene that is important for mitochondrial oxidative function in C2C12 myotubes *in vitro* (32). Perm1 is also induced in skeletal muscle by endurance exercise, raising the hypothesis that it plays a role in the enhanced oxidative capacity seen in response to exercise *in vivo*. Consistent with this hypothesis, we show here that increasing the levels of Perm1 in skeletal muscle postnatally is sufficient to enhance mitochondrial content and oxidative capacity. Moreover, Perm1 enhances muscle vascularization and resistance to fatigue, without affecting fiber-type composition. Future studies using loss-of-function approaches will be needed to determine the extent to which Perm1 is required for specific endurance exercise adaptations.

Increasing Perm1 levels in skeletal muscle for ~4 wk led to significant enhancements of mitochondrial content and oxidative function, comparable to those seen in mice in response to endurance training (39) or in transgenic mice overexpressing upstream regulators of Perm1 (*e.g.*, PGC-1α, PGC-1β, or ERRγ) or other regulators of oxidative capacity [*e.g.*, PPARδ or members of the NR4A subfamily of nuclear receptors (20, 21, 23, 24, 41, 50)]. It is noteworthy that the increased oxidative capacity of muscles over-expressing Perm1 did not alter basal levels of respiration in myofibers, suggesting that Perm1 does not affect the ATP demands of resting muscle. Rather, Perm1 selectively enhanced the spare respiratory capacity (*i.e.*, the ability of fibers to supply ATP at times of high energy demand), suggesting that muscles with high Perm1 expression use a lower fraction of their mitochondrial reserve to perform similar work as control muscles (51). The enhanced respiratory capacity is probably due to increases in both mitochondrial content and enzymatic activities. The increase in mitochondrial content may be driven by the enhanced expression of *Tfam*, *Tfb2m*, and *Endog*, which interact with the mitochondrial genome and control mitochondrial mass (52, 53). Enhancements in enzymatic activities may be driven by the increase in mitochondrial Sirt3, which deacetylates and activates SDH and other subunits of OxPhos complexes, and fatty acid oxidation enzymes (54, 55).

Besides enhancing mitochondrial content and oxidative capacity, increased Perm1 levels led to other muscle adaptations typically seen in response to endurance exercise, including enhanced vascularization, myoglobin content, and resistance to fatigue. These changes suggest that Perm1 promotes angiogenesis and oxygen transport, to meet the increased muscle oxidative capacity. The increase in vascularization is reminiscent of changes seen in mice with muscle-specific overexpression of PGC-1α, PGC-1β, or ERRγ, suggesting that PGC-1, ERRs, and Perm1 act coordinately to remodel skeletal muscle (15–17). As in these other models, Perm1 led to increased expression of *Vegfa*, a gene important for angiogenesis. The increase in *ex vivo* fatigue resistance in isolated EDL muscles over-expressing Perm1 is likely related to the increased mitochondrial oxidative capacity (56). It is also possible that Perm1 remodels other muscle pathways that contribute to fatigue mechanisms, such as, for example, Ca^{2+} handling. Future studies will need to address this.

Increased Perm1 levels in muscle led to enhancements in the expression of genes that regulate mitochondrial biogenesis and function (*Tfam*, *Tf2bm*, *Endog*, and *Sirt3*), angiogenesis (*Vegfa*), and substrate metabolism (*Glut4* and *Cpt1b*). These genes are known to be under the control of

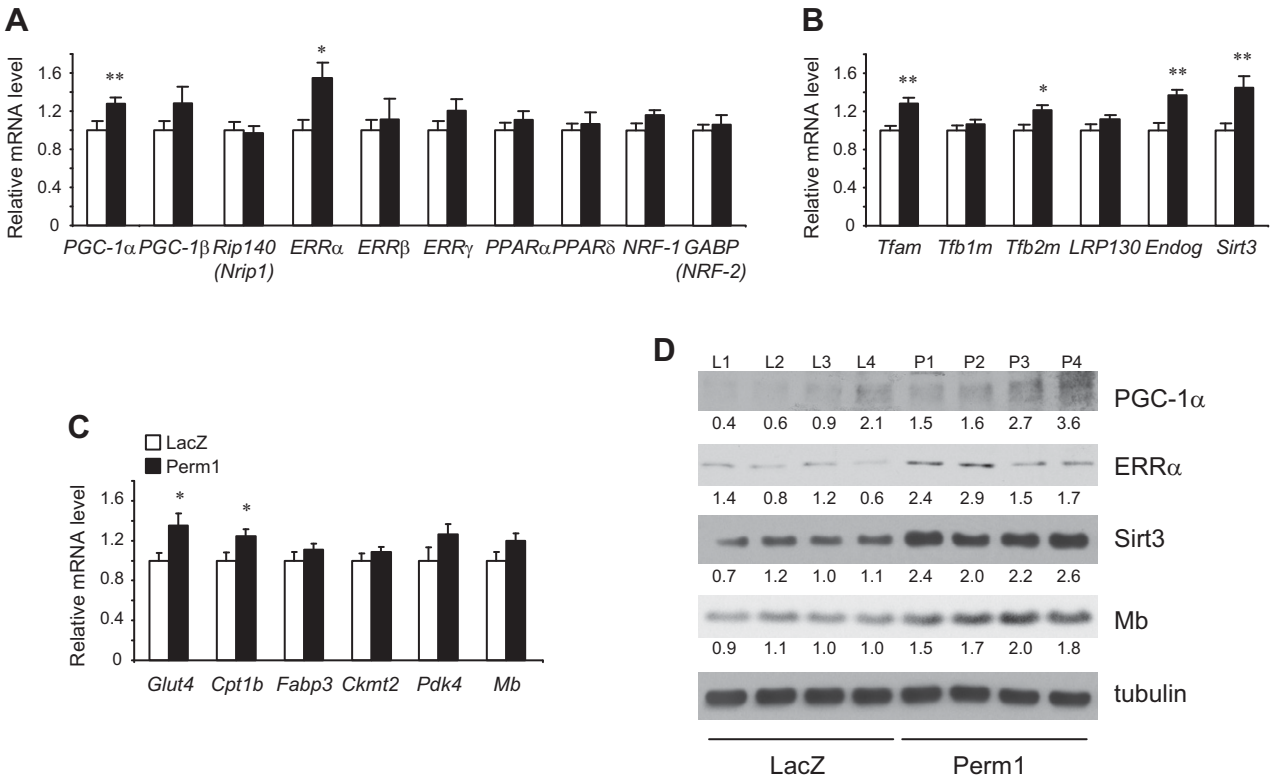

Figure 6. Increased expression of Perm1 enhances the expression of genes important for mitochondrial biogenesis and oxidative function. Total RNA was harvested from whole LacZ and Perm1 TA muscles. *A–C*) RNA levels for the indicated genes were determined by RT-quantitative PCR, normalized to GAPDH levels, and expressed relative to the levels of each gene in control (LacZ) muscles. Note that the primers used to quantify PGC-1α expression detect all PGC-1α isoforms, and it is thus unclear whether Perm1 affects differentially the different isoforms (47–49). Data are the means ± SE ($n = 14$). *$P < 0.05$; **$P < 0.01$. *D*) Protein levels of PGC-1α, ERRα, Sirt3, and myoglobin (Mb) were determined by Western blot analysis of whole TA muscles from 4 mice, expressing LacZ (L1–L4) or Perm1 (P1–P4, with numbers indicating contralateral muscles from the same mouse). The intensity of the bands was quantified using ImageJ software, normalized to the loading control (tubulin), and is indicated below each lane [expressed relative to the mean signal intensity in control (LacZ) muscles]. Note that the anti-PGC-1α antibody detects a protein isoform of ~115 kDa, corresponding to full-length PGC-1α (also called PGC-1α1) (48, 49).

multiple nuclear transcriptional regulators, including PGC-1α, PGC-1β, NRF1, GABP, PPARα, PPARδ, and ERRs (13–15, 53–55). Perm1 also led to enhanced levels of PGC-1α and ERRα, suggesting that the effects of Perm1 on gene expression are at least in part mediated through increases in these transcriptional regulators. Hence, whereas our initial observation that Perm1 is induced by PGC-1 and ERRs suggested that Perm1 acts as a downstream effector of PGC-1/ERR signaling (32), our current study shows that Perm1 can also act upstream of PGC-1/ERRs, by enhancing the expression (and possibly activity) of PGC-1α and ERRα. This finding suggests the presence of a feed-forward regulatory loop, reminiscent of what has been shown for PGC-1α and other regulators (*e.g.*, Mef2 factors) in skeletal muscle (13, 26). Based on these reciprocal interactions, we propose that the regulatory system controlling muscle oxidative capacity may be better viewed not as a linear pathway but rather as a network of interacting factors, where PGC-1α and ERRs induce the transcription of Perm1, and Perm1 promotes the expression of PGC-1α and ERRα, thereby leading to long-term adaptive changes in skeletal muscle.

The exact molecular mechanism by which Perm1 leads to changes in gene expression is currently unclear. The Perm1 protein is predominantly cytoplasmic, does not harbor a transcriptional function, and does not physically interact with PGC-1α or ERRα (32). Hence, we tested the possibility that Perm1 impacts on signaling pathways that control the activity of PGC-1 or ERR proteins. Although we did not see changes in the AMPK pathway, we observed that the increased Perm1 levels led to the activation of p38 MAPK during nighttime, when mice are physically active. We also found that acute expression of Perm1 in primary myotubes activated p38, suggesting that this activation is an early event in Perm1 action. The p38 MAPK gets activated in response to muscle contraction, and p38 activity in skeletal muscle is essential for exercise-induced PGC-1α expression and mitochondrial biogenesis (57, 58). Moreover, p38 phosphorylates and activates the PGC-1α protein and may thus act to drive a feed-forward loop of increased PGC-1α activity leading to higher PGC-1α gene expression (25, 26, 59, 60). Accordingly, it seems plausible that the Perm1-induced increase in muscle phospho-p38 activates the PGC-1α protein, resulting in enhanced PGC-1α/ERRα expression and mitochondrial biogenesis. Interestingly, the increase in p38 activity is not seen during the day, when mice rest. This

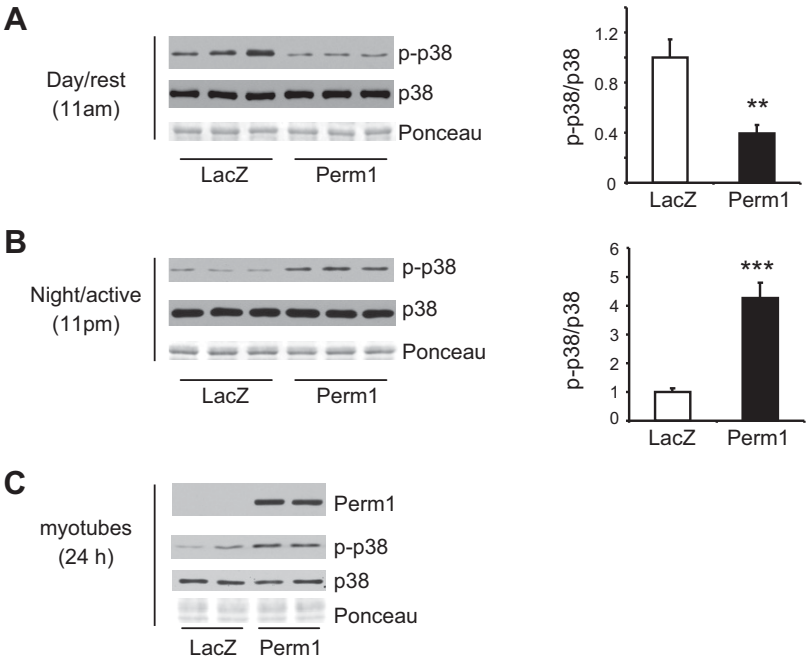

Figure 7. Perm1 modulates the active state of p38 MAPK. The levels of total and phospho-p38 MAPK in control (LacZ) and Perm1 TA muscles dissected at 11 AM [Day/rest phase in (*A*)] or 11 PM [Night/active phase of the day in (*B*)] were determined by Western blot analysis. To the right of each Western blot, the graph presents the relative levels of phospho-p38/total p38 in Day/rest phase (based on 11 AM and 3 PM) and in Night/active phase (based on 11 PM and 3 AM), quantified from the Western blots in (*A*), (*B*), and Supplemental Fig. 4*A*, and using ImageJ software. Data are the means ± SD and expressed relative to the signal intensity in control (LacZ) muscles ($n = 6$). $^{**}P < 0.01$; $^{***}P < 0.001$. *C*) The levels of total and phospho-p38 MAPK in primary myotubes infected with adenoviruses expressing control (LacZ) or Perm1 for 24 h were determined by Western blot analysis. *A–C*) Ponceau staining is shown as control for loading.

may reflect a need for other signals besides Perm1 for the activation of p38 at night, and/or the presence of lower cellular stress during the resting phase in muscles over-expressing Perm1 (likely due to the higher spare respiratory capacity); similar decreases in phospho-p38 are seen in skeletal muscles that over-express PGC-1α (61). The decreased p38 activity during the rest phase may protect the muscle from negative effects associated with chronic p38 activation (62). We still have no molecular explanation of how Perm1 activates p38. Efforts to identify binding partners of Perm1 may provide mechanistic insights into its molecular function.

Several studies suggest close regulatory links between mitochondrial oxidative function and muscle fiber-type composition. Endurance exercise training increases mitochondrial biogenesis and also promotes fiber-type switching from type IIb to IIx and to IIa (1, 4). Furthermore, in many transgenic mouse models, an increase in muscle mitochondrial oxidative capacity is associated with a shift to a more oxidative muscle fiber-type composition. For example, mice with muscle-specific overexpression of PGC-1α, PGC-1β, PPARδ, or ERRγ have increases in type I, IIa, or IIx fibers, at the expense of IIb fibers (with each transgenic model showing distinct patterns of fiber-type composition) (20–24, 63). Some of these mouse models also show decreases in fiber cross-sectional area, consistent with a switch to more oxidative fibers (21, 23). In contrast, muscles with increased Perm1 expression show enhanced mitochondrial content and oxidative capacity, but no changes in fiber-type composition. Perm1 overexpression also does not affect fiber cross-sectional area,

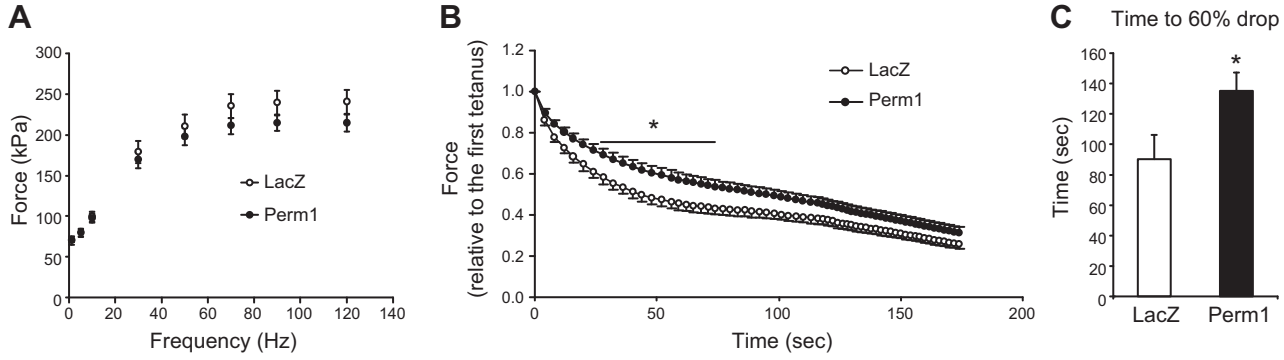

Figure 8. Increased Perm1 expression enhances fatigue resistance in skeletal muscle. *A*) Specific force generated at different frequency stimulations of EDL muscles injected with AAV1-LacZ (control) or AAV1-Perm1. Other contractile properties of the muscles are shown in Table 2. *B*) Relative force generation of LacZ and Perm1 EDL muscles during repeated stimulation for 3 min (with rest intervals between stimulations of 4 s for the first minute, 3 s for the second minute, and 2 s for the third minute). Fatigue curves were obtained from control (LacZ) or Perm1 EDL muscles. Force is expressed relative to force generated in the first contraction for each muscle. *C*) Time to fatigue is defined here as time taken for each muscle to reach 40% of the force generated in the first contraction. Data are the means ± SE ($n = 8$). $^{*}P < 0.05$.

TABLE 2. *Contractile properties of LacZ- and Perm1-transduced EDL muscles*

	LacZ	Perm1
Muscle weight (mg)	4.44 ± 0.16	4.23 ± 0.11
L_0 (mm)	10.09 ± 0.18	9.95 ± 0.16
P_0 (kPa)	244.43 ± 14.00	216.45 ± 10.01
Pt (kPa)	71.04 ± 3.94	70.37 ± 3.50
TPT (ms)	26.75 ± 0.90	25.25 ± 0.70
$RT_{1/2}$ (ms)	63.88 ± 6.11	65.00 ± 4.87
F_{50} (Hz)	25.21 ± 1.70	23.33 ± 0.98

Data are the means ± SE. F_{50}, frequency to evoke 50% of maximal tetanic force; L_0, length that promotes maximal isometric tension; P_0, specific maximal isometric tetanic force; Pt, specific twitch peak force; $RT_{1/2}$, twitch half-relaxation time; TPT, time to peak twitch tension. kPa, kilopascal.

contractile twitch properties, the force-frequency relationship, or maximal tetanic force. The lack of impact of Perm1 on muscle fiber-type composition is surprising, given the increase in PGC-1α, which is known to increase type I and IIa fibers (20). Possibly, the increase in PGC-1α expression in our Perm1 model is much more moderate than the one achieved in PGC-1α transgenic mice, thereby leading to the activation of a subset of pathways that can be activated by PGC-1α. In addition, the timing of PGC-1α increase (postnatally in our model *versus* throughout development in the PGC-1α transgenic mice) and/or posttranslational modifications of PGC-1α (*via* the altered p38 signaling in Perm1-expressing mice) may restrict PGC-1α action at select target genes. Notably, mice lacking muscle p38γ also show defects specifically in mitochondrial biogenesis and not in fiber-type switching in response to training (58). Moreover, mice that express the gain-of-function R225Q mutant of the AMPK γ3 subunit show a selective enhancement of oxidative activity, with no changes in fiber-type composition (64). Thus, it seems likely that Perm1 (like p38γ and the R225Q mutant AMPK γ3) regulates a select subset of pathways that respond to exercise.

Endurance exercise is an effective way of improving muscle performance and metabolic health, with some of the beneficial effects attributed to enhanced skeletal muscle oxidative capacity (1). Consistent with this notion, muscle-specific expression of PGC-1α or ERRγ transgenes enhances mitochondrial oxidative capacity, ameliorates symptoms of diseases affecting muscle health, and delays age-related loss of muscle function (6–9). Perm1 provides an alternate means for enhancing mitochondrial oxidative capacity, likely having overlapping but not identical actions to those of PGC-1α and ERRγ. Future experiments will determine the capacity of Perm1 to improve muscle function in mouse disease models. FJ

The authors thank Erica Young, Dr. Marin Gantner, and members of the Saez lab for technical help and discussions; Dr. Espen Spangenburg (University of Maryland, College Park, MD, USA) for help and discussions on the study of single FDB fibers; Mary Esparza and Shannon Bremner for technical assistance; Dr. Malcolm Wood (The Scripps Research Institute) for the electron microscopy studies; and Drs. Erin Brown and Shizuko Tachibana for helpful discussions and critical reading of the manuscript. This work was supported by U.S. National Institutes of Health (NIH) and American Heart Association awards: American Heart Association 12POST8610009 and 14SDG17790005 to Y.C.; American Heart Association 14POST20450112 to P.G.G.; NIH/National Institute of Diabetes and Digestive and Kidney Diseases R01DK095686 to A.K.; NIH/National Institute of Arthritis and Musculoskeletal and Skin Diseases P30AR061303; and NIH/National Institute of Child Health and Human Development R24 HD050837.

REFERENCES

1. Hawley, J. A., Hargreaves, M., Joyner, M. J., and Zierath, J. R. (2014) Integrative biology of exercise. *Cell* **159**, 738–749
2. Lexell, J. (1995) Human aging, muscle mass, and fiber type composition. *J. Gerontol. A Biol. Sci. Med. Sci.* **50**, 11–16
3. Kuznetsov, A. V., Winkler, K., Wiedemann, F. R., von Bossanyi, P., Dietzmann, K., and Kunz, W. S. (1998) Impaired mitochondrial oxidative phosphorylation in skeletal muscle of the dystrophin-deficient mdx mouse. *Mol. Cell. Biochem.* **183**, 87–96
4. Schiaffino, S., and Reggiani, C. (2011) Fiber types in mammalian skeletal muscles. *Physiol. Rev.* **91**, 1447–1531
5. Russell, A. P., Foletta, V. C., Snow, R. J., and Wadley, G. D. (2014) Skeletal muscle mitochondria: a major player in exercise, health and disease. *Biochim. Biophys. Acta* **1840**, 1276–1284
6. Handschin, C., Kobayashi, Y. M., Chin, S., Seale, P., Campbell, K. P., and Spiegelman, B. M. (2007) PGC-1alpha regulates the neuromuscular junction program and ameliorates Duchenne muscular dystrophy. *Genes Dev.* **21**, 770–783
7. Wenz, T., Diaz, F., Spiegelman, B. M., and Moraes, C. T. (2008) Activation of the PPAR/PGC-1alpha pathway prevents a bioenergetic deficit and effectively improves a mitochondrial myopathy phenotype. *Cell Metab.* **8**, 249–256
8. Wenz, T., Rossi, S. G., Rotundo, R. L., Spiegelman, B. M., and Moraes, C. T. (2009) Increased muscle PGC-1alpha expression protects from sarcopenia and metabolic disease during aging. *Proc. Natl. Acad. Sci. USA* **106**, 20405–20410
9. Matsakas, A., Yadav, V., Lorca, S., and Narkar, V. (2013) Muscle ERRγ mitigates Duchenne muscular dystrophy via metabolic and angiogenic reprogramming. *FASEB J.* **27**, 4004–4016
10. Olson, E. N., and Williams, R. S. (2000) Calcineurin signaling and muscle remodeling. *Cell* **101**, 689–692
11. Rose, A. J., and Hargreaves, M. (2003) Exercise increases Ca2+-calmodulin-dependent protein kinase II activity in human skeletal muscle. *J. Physiol.* **553**, 303–309
12. Sakamoto, K., and Goodyear, L. J. (2002) Invited review: intracellular signaling in contracting skeletal muscle. *J. Appl. Physiol.* **93**, 369–383
13. Hock, M. B., and Kralli, A. (2009) Transcriptional control of mitochondrial biogenesis and function. *Annu. Rev. Physiol.* **71**, 177–203
14. Scarpulla, R. C., Vega, R. B., and Kelly, D. P. (2012) Transcriptional integration of mitochondrial biogenesis. *Trends Endocrinol. Metab.* **23**, 459–466
15. Arany, Z., Foo, S. Y., Ma, Y., Ruas, J. L., Bommi-Reddy, A., Girnun, G., Cooper, M., Laznik, D., Chinsomboon, J., Rangwala, S. M., Baek, K. H., Rosenzweig, A., and Spiegelman, B. M. (2008) HIF-independent regulation of VEGF and angiogenesis by the transcriptional coactivator PGC-1alpha. *Nature* **451**, 1008–1012
16. Chinsomboon, J., Ruas, J., Gupta, R. K., Thom, R., Shoag, J., Rowe, G. C., Sawada, N., Raghuram, S., and Arany, Z. (2009) The transcriptional coactivator PGC-1alpha mediates exercise-induced angiogenesis in skeletal muscle. *Proc. Natl. Acad. Sci. USA* **106**, 21401–21406
17. Narkar, V. A., Fan, W., Downes, M., Yu, R. T., Jonker, J. W., Alaynick, W. A., Banayo, E., Karunasiri, M. S., Lorca, S., and Evans, R. M. (2011) Exercise and PGC-1α-independent synchronization of type I muscle metabolism and vasculature by ERRγ. *Cell Metab.* **13**, 283–293
18. Chin, E. R., Olson, E. N., Richardson, J. A., Yang, Q., Humphries, C., Shelton, J. M., Wu, H., Zhu, W., Bassel-Duby, R., and Williams, R. S. (1998) A calcineurin-dependent transcriptional pathway controls skeletal muscle fiber type. *Genes Dev.* **12**, 2499–2509

19. Calabria, E., Ciciliot, S., Moretti, I., Garcia, M., Picard, A., Dyar, K. A., Pallafacchina, G., Tothova, J., Schiaffino, S., and Murgia, M. (2009) NFAT isoforms control activity-dependent muscle fiber type specification. *Proc. Natl. Acad. Sci. USA* **106**, 13335–13340
20. Lin, J., Wu, H., Tarr, P. T., Zhang, C. Y., Wu, Z., Boss, O., Michael, L. F., Puigserver, P., Isotani, E., Olson, E. N., Lowell, B. B., Bassel-Duby, R., and Spiegelman, B. M. (2002) Transcriptional co-activator PGC-1 alpha drives the formation of slow-twitch muscle fibres. *Nature* **418**, 797–801
21. Rangwala, S. M., Wang, X., Calvo, J. A., Lindsley, L., Zhang, Y., Deyneko, G., Beaulieu, V., Gao, J., Turner, G., and Markovits, J. (2010) Estrogen-related receptor gamma is a key regulator of muscle mitochondrial activity and oxidative capacity. *J. Biol. Chem.* **285**, 22619–22629
22. Gan, Z., Rumsey, J., Hazen, B. C., Lai, L., Leone, T. C., Vega, R. B., Xie, H., Conley, K. E., Auwerx, J., Smith, S. R., Olson, E. N., Kralli, A., and Kelly, D. P. (2013) Nuclear receptor/microRNA circuitry links muscle fiber type to energy metabolism. *J. Clin. Invest.* **123**, 2564–2575
23. Arany, Z., Lebrasseur, N., Morris, C., Smith, E., Yang, W., Ma, Y., Chin, S., and Spiegelman, B. M. (2007) The transcriptional coactivator PGC-1beta drives the formation of oxidative type IIX fibers in skeletal muscle. *Cell Metab.* **5**, 35–46
24. Wang, Y. X., Zhang, C. L., Yu, R. T., Cho, H. K., Nelson, M. C., Bayuga-Ocampo, C. R., Ham, J., Kang, H., and Evans, R. M. (2004) Regulation of muscle fiber type and running endurance by PPARdelta. *PLoS Biol.* **2**, e294
25. Akimoto, T., Pohnert, S. C., Li, P., Zhang, M., Gumbs, C., Rosenberg, P. B., Williams, R. S., and Yan, Z. (2005) Exercise stimulates Pgc-1alpha transcription in skeletal muscle through activation of the p38 MAPK pathway. *J. Biol. Chem.* **280**, 19587–19593
26. Handschin, C., Rhee, J., Lin, J., Tarr, P. T., and Spiegelman, B. M. (2003) An autoregulatory loop controls peroxisome proliferator-activated receptor gamma coactivator 1alpha expression in muscle. *Proc. Natl. Acad. Sci. USA* **100**, 7111–7116
27. Schuler, M., Ali, F., Chambon, C., Duteil, D., Bornert, J. M., Tardivel, A., Desvergne, B., Wahli, W., Chambon, P., and Metzger, D. (2006) PGC1alpha expression is controlled in skeletal muscles by PPARbeta, whose ablation results in fiber-type switching, obesity, and type 2 diabetes. *Cell Metab.* **4**, 407–414
28. Hondares, E., Pineda-Torra, I., Iglesias, R., Staels, B., Villarroya, F., and Giralt, M. (2007) PPARdelta, but not PPARalpha, activates PGC-1alpha gene transcription in muscle. *Biochem. Biophys. Res. Commun.* **354**, 1021–1027
29. Schreiber, S. N., Knutti, D., Brogli, K., Uhlmann, T., and Kralli, A. (2003) The transcriptional coactivator PGC-1 regulates the expression and activity of the orphan nuclear receptor estrogen-related receptor alpha (ERRalpha). *J. Biol. Chem.* **278**, 9013–9018
30. Huss, J. M., Torra, I. P., Staels, B., Giguère, V., and Kelly, D. P. (2004) Estrogen-related receptor alpha directs peroxisome proliferator-activated receptor alpha signaling in the transcriptional control of energy metabolism in cardiac and skeletal muscle. *Mol. Cell. Biol.* **24**, 9079–9091
31. Mootha, V. K., Handschin, C., Arlow, D., Xie, X., St Pierre, J., Sihag, S., Yang, W., Altshuler, D., Puigserver, P., Patterson, N., Willy, P. J., Schulman, I. G., Heyman, R. A., Lander, E. S., and Spiegelman, B. M. (2004) Erralpha and Gabpa/b specify PGC-1alpha-dependent oxidative phosphorylation gene expression that is altered in diabetic muscle. *Proc. Natl. Acad. Sci. USA* **101**, 6570–6575
32. Cho, Y., Hazen, B. C., Russell, A. P., and Kralli, A. (2013) Peroxisome proliferator-activated receptor γ coactivator 1 (PGC-1)- and estrogen-related receptor (ERR)-induced regulator in muscle 1 (Perm1) is a tissue-specific regulator of oxidative capacity in skeletal muscle cells. *J. Biol. Chem.* **288**, 25207–25218
33. Timmons, J. A., Wennmalm, K., Larsson, O., Walden, T. B., Lassmann, T., Petrovic, N., Hamilton, D. L., Gimeno, R. E., Wahlestedt, C., Baar, K., Nedergaard, J., and Cannon, B. (2007) Myogenic gene expression signature establishes that brown and white adipocytes originate from distinct cell lineages. *Proc. Natl. Acad. Sci. USA* **104**, 4401–4406
34. Minamoto, V. B., Hulst, J. B., Lim, M., Peace, W. J., Bremner, S. N., Ward, S. R., and Lieber, R. L. (2007) Increased efficacy and decreased systemic-effects of botulinum toxin A injection after active or passive muscle manipulation. *Dev. Med. Child Neurol.* **49**, 907–914
35. Gokhin, D. S., and Fowler, V. M. (2011) Cytoplasmic gamma-actin and tropomodulin isoforms link to the sarcoplasmic reticulum in skeletal muscle fibers. *J. Cell Biol.* **194**, 105–120
36. Tiraby, C., Hazen, B. C., Gantner, M. L., and Kralli, A. (2011) Estrogen-related receptor gamma promotes mesenchymal-to-epithelial transition and suppresses breast tumor growth. *Cancer Res.* **71**, 2518–2528
37. Villena, J. A., Hock, M. B., Chang, W. Y., Barcas, J. E., Giguère, V., and Kralli, A. (2007) Orphan nuclear receptor estrogen-related receptor alpha is essential for adaptive thermogenesis. *Proc. Natl. Acad. Sci. USA* **104**, 1418–1423
38. Schreiber, S. N., Emter, R., Hock, M. B., Knutti, D., Cardenas, J., Podvinec, M., Oakeley, E. J., and Kralli, A. (2004) The estrogen-related receptor alpha (ERRalpha) functions in PPARgamma coactivator 1alpha (PGC-1alpha)-induced mitochondrial biogenesis. *Proc. Natl. Acad. Sci. USA* **101**, 6472–6477
39. Philp, A., Chen, A., Lan, D., Meyer, G. A., Murphy, A. N., Knapp, A. E., Olfert, I. M., McCurdy, C. E., Marcotte, G. R., Hogan, M. C., Baar, K., and Schenk, S. (2011) Sirtuin 1 (SIRT1) deacetylase activity is not required for mitochondrial biogenesis or peroxisome proliferator-activated receptor-gamma coactivator-1alpha (PGC-1alpha) deacetylation following endurance exercise. *J. Biol. Chem.* **286**, 30561–30570
40. Talmadge, R. J., and Roy, R. R. (1993) Electrophoretic separation of rat skeletal muscle myosin heavy-chain isoforms. *J. Appl. Physiol.* **75**, 2337–2340
41. Pearen, M. A., Eriksson, N. A., Fitzsimmons, R. L., Goode, J. M., Martel, N., Andrikopoulos, S., and Muscat, G. E. (2012) The nuclear receptor, Nor-1, markedly increases type II oxidative muscle fibers and resistance to fatigue. *Mol. Endocrinol.* **26**, 372–384
42. Schuh, R. A., Jackson, K. C., Khairallah, R. J., Ward, C. W., and Spangenburg, E. E. (2012) Measuring mitochondrial respiration in intact single muscle fibers. *Am. J. Physiol. Regul. Integr. Comp. Physiol.* **302**, R712–R719
43. Mokbel, N., Ilkovski, B., Kreissl, M., Memo, M., Jeffries, C. M., Marttila, M., Lehtokari, V. L., Lemola, E., Grönholm, M., Yang, N., Menard, D., Marcorelles, P., Echaniz-Laguna, A., Reimann, J., Vainzof, M., Monnier, N., Ravenscroft, G., McNamara, E., Nowak, K. J., Laing, N. G., Wallgren-Pettersson, C., Trewhella, J., Marston, S., Ottenheijm, C., North, K. N., and Clarke, N. F. (2013) K7del is a common TPM2 gene mutation associated with nemaline myopathy and raised myofibre calcium sensitivity. *Brain* **136**, 494–507
44. Chleboun, G. S., Patel, T. J., and Lieber, R. L. (1997) Skeletal muscle architecture and fiber-type distribution with the multiple bellies of the mouse extensor digitorum longus muscle. *Acta Anat. (Basel)* **159**, 147–155
45. Schild, M., Ruhs, A., Beiter, T., Zügel, M., Hudemann, J., Reimer, A., Krumholz-Wagner, I., Wagner, C., Keller, J., Eder, K., Krüger, K., Krüger, M., Braun, T., Nieß, A., Steinacker, J., and Mooren, F. C. (2015) Basal and exercise induced label-free quantitative protein profiling of m. vastus lateralis in trained and untrained individuals. *J. Proteomics* **122**, 119–132
46. Louboutin, J. P., Wang, L., and Wilson, J. M. (2005) Gene transfer into skeletal muscle using novel AAV serotypes. *J. Gene Med.* **7**, 442–451
47. Miura, S., Kai, Y., Kamei, Y., and Ezaki, O. (2008) Isoform-specific increases in murine skeletal muscle peroxisome proliferator-activated receptor-gamma coactivator-1alpha (PGC-1alpha) mRNA in response to beta2-adrenergic receptor activation and exercise. *Endocrinology* **149**, 4527–4533
48. Zhang, Y., Huypens, P., Adamson, A. W., Chang, J. S., Henagan, T. M., Boudreau, A., Lenard, N. R., Burk, D., Klein, J., Perwitz, N., Shin, J., Fasshauer, M., Kralli, A., and Gettys, T. W. (2009) Alternative mRNA splicing produces a novel biologically active short isoform of PGC-1alpha. *J. Biol. Chem.* **284**, 32813–32826
49. Ruas, J. L., White, J. P., Rao, R. R., Kleiner, S., Brannan, K. T., Harrison, B. C., Greene, N. P., Wu, J., Estall, J. L., Irving, B. A., Lanza, I. R., Rasbach, K. A., Okutsu, M., Nair, K. S., Yan, Z., Leinwand, L. A., and Spiegelman, B. M. (2012) A PGC-1α isoform induced by resistance training regulates skeletal muscle hypertrophy. *Cell* **151**, 1319–1331
50. Chao, L. C., Wroblewski, K., Ilkayeva, O. R., Stevens, R. D., Bain, J., Meyer, G. A., Schenk, S., Martinez, L., Vergnes, L., Narkar, V. A., Drew, B. G., Hong, C., Boyadjian, R., Hevener, A. L., Evans, R. M., Reue, K., Spencer, M. J., Newgard, C. B., and Tontonoz, P. (2012)

Skeletal muscle Nur77 expression enhances oxidative metabolism and substrate utilization. *J. Lipid Res.* **53**, 2610–2619
51. Brand, M. D., and Nicholls, D. G. (2011) Assessing mitochondrial dysfunction in cells. *Biochem. J.* **435**, 297–312
52. Larsson, N. G., Wang, J., Wilhelmsson, H., Oldfors, A., Rustin, P., Lewandoski, M., Barsh, G. S., and Clayton, D. A. (1998) Mitochondrial transcription factor A is necessary for mtDNA maintenance and embryogenesis in mice. *Nat. Genet.* **18**, 231–236
53. McDermott-Roe, C., Ye, J., Ahmed, R., Sun, X. M., Serafín, A., Ware, J., Bottolo, L., Muckett, P., Cañas, X., Zhang, J., Rowe, G. C., Buchan, R., Lu, H., Braithwaite, A., Mancini, M., Hauton, D., Martí, R., García-Arumí, E., Hubner, N., Jacob, H., Serikawa, T., Zidek, V., Papousek, F., Kolar, F., Cardona, M., Ruiz-Meana, M., García-Dorado, D., Comella, J. X., Felkin, L. E., Barton, P. J., Arany, Z., Pravenec, M., Petretto, E., Sanchis, D., and Cook, S. A. (2011) Endonuclease G is a novel determinant of cardiac hypertrophy and mitochondrial function. *Nature* **478**, 114–118
54. Brenmoehl, J., and Hoeflich, A. (2013) Dual control of mitochondrial biogenesis by sirtuin 1 and sirtuin 3. *Mitochondrion* **13**, 755–761
55. Giralt, A., and Villarroya, F. (2012) SIRT3, a pivotal actor in mitochondrial functions: metabolism, cell death and aging. *Biochem. J.* **444**, 1–10
56. Allen, D. G., Lamb, G. D., and Westerblad, H. (2008) Skeletal muscle fatigue: cellular mechanisms. *Physiol. Rev.* **88**, 287–332
57. Gibala, M. J., McGee, S. L., Garnham, A. P., Howlett, K. F., Snow, R. J., and Hargreaves, M. (2009) Brief intense interval exercise activates AMPK and p38 MAPK signaling and increases the expression of PGC-1alpha in human skeletal muscle. *J. Appl. Physiol.* **106**, 929–934
58. Pogozelski, A. R., Geng, T., Li, P., Yin, X., Lira, V. A., Zhang, M., Chi, J. T., and Yan, Z. (2009) p38gamma mitogen-activated protein kinase is a key regulator in skeletal muscle metabolic adaptation in mice. *PLoS One* **4**, e7934
59. Knutti, D., Kressler, D., and Kralli, A. (2001) Regulation of the transcriptional coactivator PGC-1 via MAPK-sensitive interaction with a repressor. *Proc. Natl. Acad. Sci. USA* **98**, 9713–9718
60. Puigserver, P., Rhee, J., Lin, J., Wu, Z., Yoon, J. C., Zhang, C. Y., Krauss, S., Mootha, V. K., Lowell, B. B., and Spiegelman, B. M. (2001) Cytokine stimulation of energy expenditure through p38 MAP kinase activation of PPARgamma coactivator-1. *Mol. Cell* **8**, 971–982
61. Selsby, J. T., Morine, K. J., Pendrak, K., Barton, E. R., and Sweeney, H. L. (2012) Rescue of dystrophic skeletal muscle by PGC-1α involves a fast to slow fiber type shift in the mdx mouse. *PLoS One* **7**, e30063
62. Wang, Y., Huang, S., Sah, V. P., Ross, Jr., J., Brown, J. H., Han, J., and Chien, K. R. (1998) Cardiac muscle cell hypertrophy and apoptosis induced by distinct members of the p38 mitogen-activated protein kinase family. *J. Biol. Chem.* **273**, 2161–2168
63. Matsakas, A., Yadav, V., Lorca, S., Evans, R. M., and Narkar, V. A. (2012) Revascularization of ischemic skeletal muscle by estrogen-related receptor-γ. *Circ. Res.* **110**, 1087–1096
64. Garcia-Roves, P. M., Osler, M. E., Holmström, M. H., and Zierath, J. R. (2008) Gain-of-function R225Q mutation in AMP-activated protein kinase gamma3 subunit increases mitochondrial biogenesis in glycolytic skeletal muscle. *J. Biol. Chem.* **283**, 35724–35734

Received for publication May 19, 2015.
Accepted for publication September 22, 2015.